Missouri S&T Library and Learning Resources

Scholars' Mine

Masters Theses

Student Theses and Dissertations

Spring 2015

# Compressed sensing techniques for radial Ultra-short Echo Time (UTE) magnetic resonance imaging

Xiahan Yang

Follow this and additional works at: https://scholarsmine.mst.edu/masters_theses

 Part of the Electrical and Computer Engineering Commons

Department:

Recommended Citation

Yang, Xiahan, "Compressed sensing techniques for radial Ultra-short Echo Time (UTE) magnetic resonance imaging" (2015). *Masters Theses*. 7422.
https://scholarsmine.mst.edu/masters_theses/7422

This thesis is brought to you by Scholars' Mine, a service of the Missouri S&T Library and Learning Resources. This work is protected by U. S. Copyright Law. Unauthorized use including reproduction for redistribution requires the permission of the copyright holder. For more information, please contact scholarsmine@mst.edu.

www.manaraa.com

# COMPRESSED SENSING TECHNIQUES FOR RADIAL ULTRA-SHORT ECHO TIME (UTE) MAGENTIC RESONANCE IMAGING

by

XIAHAN YANG

A THESIS

Presented to the Faculty of the Graduate School of

MISSOURI UNIVERSITY OF SCIENCE AND TECHNOLOGY

in Partial Fulfillment of the Requirements for the Degree

MASTER OF SCIENCE IN ELECTRICAL ENGINEERING

2015

Approved by

Dr. Yahong Rosa Zheng, Advisor
Dr. Steven Grant
Dr. Randy H. Moss

www.manaraa.com

المنارة للاستشارات
www.manaraa.com

## PUBLICATION THESIS OPTION

This thesis consists of the following two published or to be published papers, formatted in the style used by the Missouri University of Science and Technology, listed as follows:

Paper I, X. Yang, Y. R. Zheng, M. Yang, and L. Ma, "Compressed Sensing with Non-Uniform Fast Fourier Transform for Radial Ultra-Short Echo Time (UTE) MRI," *2015 IEEE 12th International Symposium Biomedical Imaging (ISBI),* Brooklyn, New York, Jan. 2015, Accepted.

Paper II, X. Yang, Y. R. Zheng, and L. Ma, "Automated Cardiac Self-Gated Radial CMRI," *2015 IEEE International Symposium Medical Measurements and Applications (MeMeA),* Torino, Italy, Mar. 2015, Accepted.

www.manaraa.com

## ABSTRACT

This thesis proposes two techniques, namely Compressed Sensing (CS) and self-gating, for pre-clinical (CMRI) to reduce scan time and RF exposure to mouse heart, simply experimental procedures, and improve imaging quality. The proposed CS technique reduces the number of radial trajectories in Ultra-short Echo Time (UTE) CMRI scans on a 7 Tesla MRI machine to acquire 13% to 38% of the fully sampled k-space data. To reconstruct the image, the Non-Uniform Fast Fourier Transform (NUFFT) is utilized in each iteration of the l1-norm optimization algorithm of the CS to reduce error and aliasing. Experimental results with a phantom and a mouse heart samples show that the image quality of the proposed NUFFT-CS reconstructions, measured by the Peak Signal to Noise ratio (PSNR) and structural similarity (SSIM), is obviously better than those of traditional zero-filling method and regridding-CS method. Comparing the images of the CS technique with the reconstructions of fully sampled data, the quality degradation is illegible while the scan time is largely reduced.

The proposed self-gating technique extracts the cardiac cycle information directly from the UTE CMRI measurements that are acquired without Electrocardiography (ECG) trigger. The proposed detector filters the k0 lines in the no-trigger UTE MRI scans to extract the cardiac cycle features, and automatically detects the peaks of the filtered signal as the cycle start points. The reconstruct cardiac images based on the self-gating signals reflect the cardiac cycle clearly and the scan time in MRI exams is reduced by 40% to 70%. The proposed self-gating detector differs from existing k0-line detector in the filter design and in the combination with NUFFT image reconstruction. Future research in this direction may include thorough analysis of the detector performance and may combine self-gated MRI with CS reconstruction.

www.manaraa.com

# ACKNOWLEDGMENTS

I would like to thank Dr. Yahong Rosa Zheng, my academic advisor. Her enthusiasm and dedication towards research have always been a great source of inspiration. She has instructed me in research attitude, specific knowledge, technical writing throughout the weekly meeting, and weekly report. Thanks for her training on research skill, encouragement on academic development, and personal growth. Her advice on both research and career are priceless to me. This thesis would not have been possible without her support and guidance.

I would like to thank for the funding support in my research. I would like to thank the IDIC funding of Dr. Zheng and Dr. Ma from the MU system and the ISC funding of Dr. Zheng from the Missouri S&T to help me continue my research and support me to do the experiments.

I wish to thank Dr. Lixin Ma of the radiology department of Harry Truman Hospital for her help with MRI experiments during a 2-month stay in her lab. Her support and guidance for my research work have helped me invaluably for the MRI research. She provided a lot of technical assistance, good ideas, and research chances for me, which will help me all my life.

I would like to thank the other members of my advisory committee, Drs. Randy Moss and Steve Grant for generously offering their time and advice for my research.

www.manaraa.com

# TABLE OF CONTENTS



www.manaraa.com

# LIST OF ILLUSTRATIONS



www.manaraa.com

# LIST OF TABLES



www.manaraa.com

# 1. INTRODUCTION

Cardiovascular magnetic resonance imaging (CMRI), sometimes known as cardiac MRI, is a medical imaging technology fornon-invasive assessment of functions and structures of the cardiovascular systems. In a MRI exam, a powerful magnetic field, ratio frequency pulse sequences and a processer are necessary to exhibit the images of the bonds, cardiac, lung or other interested tissues. Researcher are working on different MRI topics like clearer reconstruction, faster scan time, more flexible parameters setting. To reach the target, a lot of experiments are necessary to record and analysis.

However, in biological research, it is impossible always do the MRI exam with human. Researcher use animals to do the test, as known as pre-clinical research. In our research, we use mice to do the CMRI. There are the obvious reasons to choose mice: they are small the easily kept, they have much commons of our biology as mammals. While the mice looks a huge different from humans, for many purposes, they are genetically close enough for human. The experiment results from the pre-clinical MRI exam with mice could provide largely useful information.

Among the CMRI research topics, an efficient and effective radio frequency pulse sequences is one of the major directions. The most popular MRI sequence applied in clinical and pre-clinical experiments is Fast Low Angel Shot (FLASH) sequence. However, in our research, we adopt a new sequence named as Ultra-short Echo Time (UTE) sequence. UTE, sequence as proposed in recent years, has developed to a powerful approach in the CMRI field [1] to replace the conventional FLASH sequence. Compared with the Flash sequence, Ultra-short Echo Time (UTE) technology could record the tissues with low $T_2$ time and perform good in susceptibility effects. The performance of UTE sequence reconstructions is much higher than the FLASH sequence in some situations, especially for preclinical experiments which often suffer from blood-flow turbulence artifact due to the rapid heart rates of the rodent animals as shown in Figure 1.1. As the arrow shown the blood-artifacts in the Figure 1.1, the UTE MRI could rebuilt a clear left-ventricular

www.manaraa.com

cardiac image in the end-diastole phase, while the FLASH MRI cannot record that time blood reflected signals and the normal left-ventricular part is blur and caliginous, without any useful information.

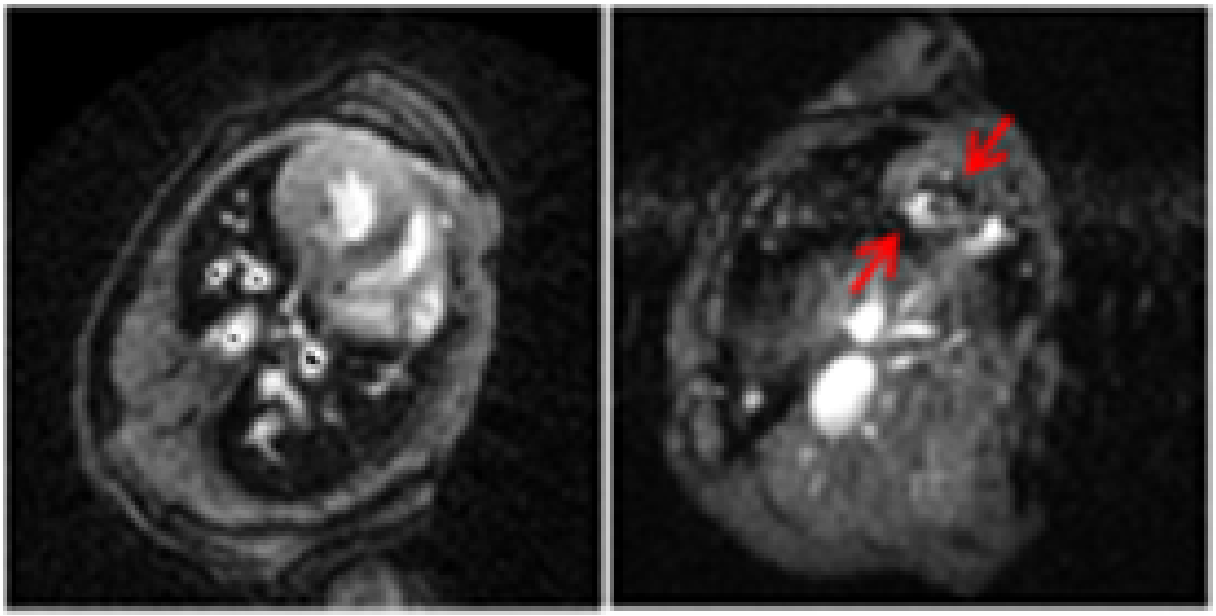

Figure 1.1: Left is the reconstruction of UTE sequence and Right is the reconstruction of FLASH sequence. Arrow shows the flow artifact

However, with the higher performance in UTE MRI, the cost and time are also higher than the FLASH sequence. Figure 1.2 shows the different physical theory and k-space trajectory between the FLASH and UTE sequence, where A. is the UTE sequence diagram used for radial cine MRI acquisition. The minimal TE can be as low as 400 s; B. is the FLASH sequence diagram used for Cartesian cine MRI acquisition. The minimal TE is 1.5ms given 10 kHz receiver bandwidth; C. is the k-space data trajectory of uniform Cartesian acquisition and D. is the k-space data trajectory of uniform radial acquisition. . From the Figure 1.2. It is obviously that more power is necessary in the RF pulse and the trajectory is radial instead of the simple Cartesian grid.

www.manaraa.com

Radial trajectory is not a simple replacement of the conventional Cartesian grid. Actually, with radial trajectory, more projections are necessary to cover the radial k-space. For example, an animal sample measurements with FOV=$3.5 \times 2.5cm^2$ and acquisition matrix = $194 \times 194$ is acquired 610 projections and 89 data points per projections for the full data acquisition in UTE sequence. When the same parameters of FOV and acquisition matrix are setup to the FLASH sequence, only 194 projections and 194 data points per projections are necessary. Moreover, with MRI theory, the processing time in one projection is as low as to ignore in MRI exam compared with the processing time for projections. For the same example, the rate of estimated time between the UTE sequence and FLASH sequence is $\frac{610}{194} = 3.1442399$. In other word, triple time is necessary in UTE sequence compared with the FLASH sequence. Therefore, it is of practical interest to reduce the acquisition time in CMRI.

In the research, we propose two different methods to save the scanning time in UTE sequence: Compressed Sensing and Self-Gating. Compressed sensing as a widely approached in MRI experiments, could help the researchers to improve the quality of reconstructions and reduce the scan time [2] [3] [4]. In compressed sensing theory, the signals can be reconstructed perfectly when the RIP condition is satisfied. With the CS approach, images can be reconstructed with under-sampled measurements, even much lower than the Nyquist-Shannon sampling rate, while the quality of the reconstruction would not be eliminated. However, as we applied the UTE sequence, the traditional compressed sensing cannot be adopted directly as the measurements are in radial trajectory. The previously algorithm to reconstructed the image from the radial trajectory is do the linear interpolation of the radial measurements to Cartesian grid first and then calculate the inverse Fourier transform to obtain the image, as known as regridding method. The quality of the reconstructions with regridding method is acceptable with the fully-sampled measurements. If we embed the regridding method in compressed sensing, the interpolated error accumulated in CS iterations would destroy the final reconstruction. To keep

www.manaraa.com

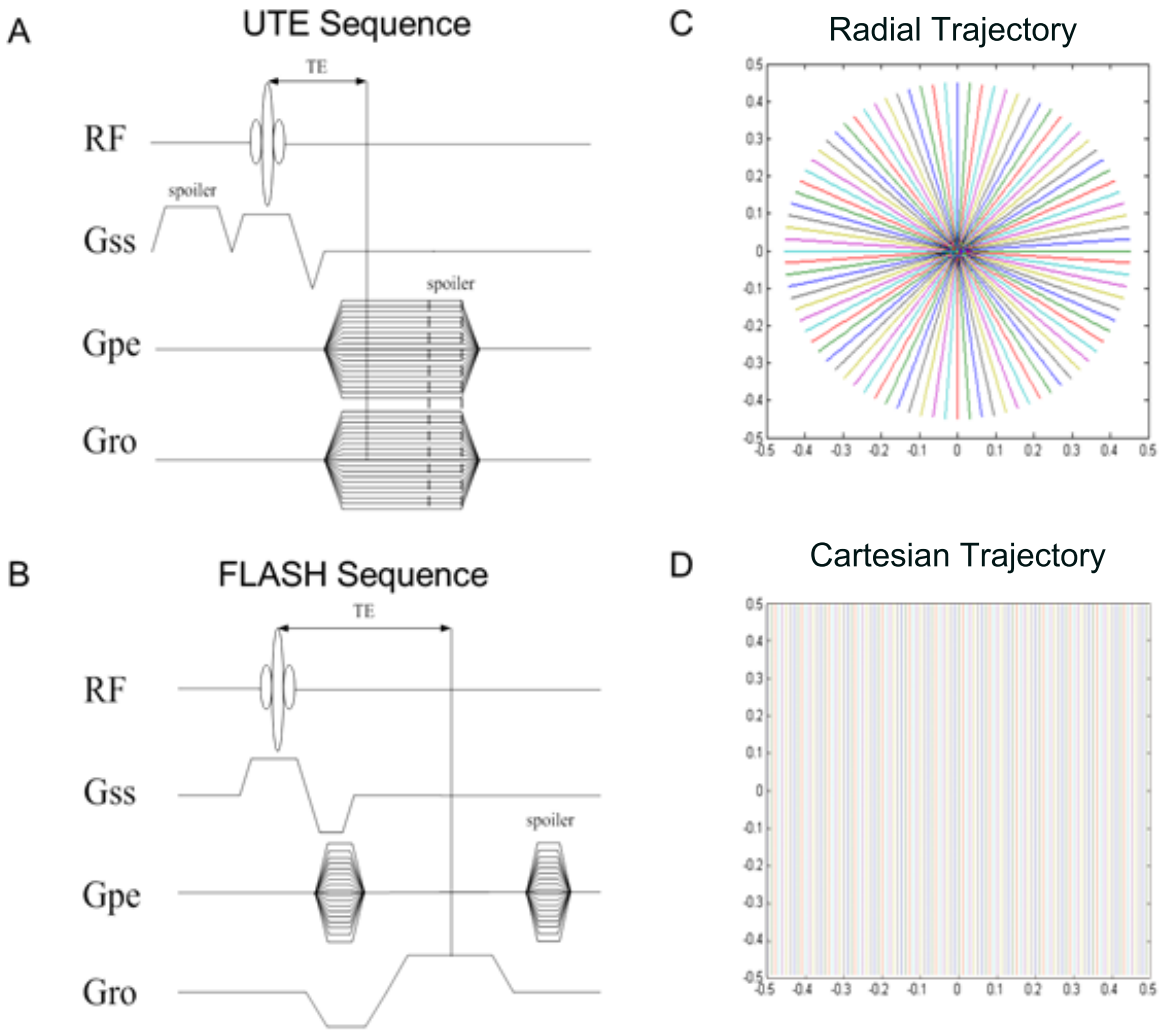


Figure 1.2: The sequence diagram and the k-space trajectory of UTE and FlASH MRI.

the low error rate in each CS iteration, we applied the NUFFT operator to replace the regridding method in the research.

The accuracy of the NUFFT algorithm is much higher than the regridding method. Different from the linear interpolation applied in the regridding, NUFFT algorithm do a non-linear interpolation with an exact kernel in the Fourier transform operator to replace the formal 2D Fast Fourier transform operator. As a non-linear algorithm, NUFFT method improve the quality of the reconstruction. Combine with the UTE technology, the improvement of the results is significantly. Embedded with the NUFFT operator,

www.manaraa.com

the error in each iteration could been highly reduced and the iteration could be finished correctly.

In the research, we compared the performance of the NUFFT-CS, Regridding-CS and zero-filling approaches. We calculate the real fully-sampled and under-sampled UTE MRI measurements as the input data. The under-sampled measurements are recorded physically from the MRI machine instead of simulated electronically. As a result, the experiment results are more accurate and reliable.

AS the compressed sensing reduce the necessary of the measurements, we also applied the self-gating approach to separate the CMRI exam from the electrocardiogram (ECG) gating signal.

The need for ECG gating signal would highly increasing the time in pre-clinical CMRI exam. The rate of cardiac cycle of mice in the pre-clinical MRI experiment is as high as 400 600 bpm. With that fast heart beating rate, the ECG trigger always cannot recorded the accuracy trigger signal which is important in the previous MRI exam. As a result, the MRI scanner have to wait the ECG trigger signal sending the correct one to continue record the measurements. The waiting time always occupy $40\%to70\%$ in the whole MRI exam time.

In the research, we adopt the Self-gating approach to eliminate the need to acquire additional gating data by extracting the motion synchronization signal directly from the k-space measurements. Many researchers have applied the self-gating technology [5] [6]. In the research, We adopted a bandpass filter with peak-detection restrictions to extract the self-gating signals. We also compared results with a common lowpass filter. Both of the reconstructions and the self-gating signals quality has been improved. The reconstructions with band-pass filter can effectively distinguish the cardiac cycle where the MRI exam time and the radiations have been significantly reduced.

Scientific contributions of this thesis include:

www.manaraa.com

1. Compressed sensing approach is successfully applied to Ultra-Short Echo-time (UTE) Magnetic Resonance Imaging (MRI) exam with low sampled measurements. Benefiting from a reduced number of samples, NUFFT approach is embedded to reconstructed the radial k-space measurement in contrast with the zero-filling and regridding approach. Experiment results show that 20% for phantom and 13% for real animal measurement are necessary with NUFFT-CS approach to rebuild high quality image.

2. Self-gating approach is successfully to replace the ECG-trigger in UTE MRI exam. Images can be reconstructed with the no-trigger measurements with the SG. Waiting time during the ECG-trigger detection has been totally eliminated.

3. In the research, all the measurements are from the real MRI exam instead of simulated electronically. With the record in MRI exam, the MRI scan time is high reduced both in the low sampling rate measurement and no-trigger measurement. Experiment results support that the compressed sensing approach and self-gating approach could save the MRI scan time.

www.manaraa.com

# I. COMPRESSED SENSING WITH NON-UNIFORM FAST FOURIER TRANSFORM FOR RADIAL ULTRA-SHORT ECHO TIME (UTE) MRI

Xiahan Yang, Yahong Rosa Zheng, Ming Yang, and Lixin Ma

**ABSTRACT**—This paper proposes a compressive sensing (CS) method for radial Magnetic Resonance Imaging (MRI) using non-uniform fast fourier transform (NUFFT). With the Ultra-short Echo Time (UTE) technology, radial MRI can reduce scan time, reduce artifacts, and achieve high imaging quality. We show that NUFFT-CS reconstruction from under-sampled radial k-space measurements achieves better image quality than the zero-filling (ZF) approaches and the existing CS approach that uses regridding. Experiments using phantom and animal samples have verified that the NUFFT-CS achieves better performance than the NUFFT-ZF, regrid-ZF, and regrid-CS, especially at small sampling rates.

www.manaraa.com

# 1. INTRODUCTION

Ultra-short Echo Time (UTE) technology exhibits great promises in Cardiac Magnetic Resonance Imaging (CMRI), especially for preclinical experiments which often suffer from blood-flow turbulence artifact due to the rapid heart rates of the rodent animals [7]. In contrast to the conventional FLASH sequence that can scan the k-space in Cartesian grid, the UTE has to acquire measurements in radial scan [8]. Therefore, image reconstruction from the radial scan is often achieved by regridding plus 2-dimensional DFT (Discrete Fourier Transform) or the Least Square Reconstruction (LSR) [9,10]. The scan time can be further reduced by using a sampling density that is less than the Nyquist rate and the Compressed Sensing (CS) techniques [3,11] are used to reconstruct the image with little performance degradation.

Existing works for radial MRI reconstruction use the CS L1 optimization in combination with regridding [12]. In this paper, the Non-Uniform Fast Fourier Transform (NUFFT) [13, 14] is used with CS to reconstruct image in Cartesian grid without interpolating the radial k-space data. Similar to the NUFFT-CS algorithms developed for the Synthetic Aperture Radar (SAR) imaging systems [15, 16], the NUFFT-CS achieves better image quality over the regrid-CS by removing interpolation errors of regridding. With Density Compensation Function (DCF) and 2D imaging, the NUFFT-CS for MRI omits the truncation repair procedure that is required in the 3D SAR imaging system. results of two experiment samples demonstrate that the NUFFT-CS is effective in reducing the sampling density while achieving high image quality.

www.manaraa.com

## 2. REGRIDDING VERSUS NUFFT

Assume the 2D radial MRI trajectory consists of $N$ projection lines with $M$ sample points per line. The total number of projections is then $N \times M$. Let $L \times L$ be the size of the reconstructed image in Cartesian grid. The sampling density is then $\eta = MN/L^2$. For cardiac MRI, multiple frames are scanned in each cardiac cycle and a data cube with multiple cycles is sliced per frame to reconstruct a 2D image. Let $f(u, v, t_0)$ be the raw k-space measurements at coordinate $(u, v)$ for frame $t_0$ and $I(x, y, t_0)$ be the image intensity at Cartesian coordinate $(x, y)$ for frame $t_0$. Note that $(u, v)$ points are nonuniform in Cartesian while $(x, y)$ points are uniform in Cartesian.

The regridding method first interpolates the nonuniform raw measurement to the uniform Cartesian grid in k-space, then applies the inverse 2DFT to transform the k-space data to image. To reduce the interpolation error, each data point is compensated by the density compensation function (DCF) before the inverse 2DFT and by the apodization function after the inverse 2DFT. The image estimated by the overall operation function of re-gridding is then [12]

$$\hat{I}_g = \mathbf{QD}^{\star}\mathbf{SPf} \tag{1}$$

where $\hat{I}_g \in \mathbb{C}^{L^2 \times 1}$ and $\mathbf{f} \in \mathbb{C}^{(MN)\times 1}$ are the vectorized image and k-space measurement, respectively, $\mathbf{P}$ is the $(MN) \times (MN)$ diagonal matrix of DCF, $\mathbf{S}$ is the $L^2 \times (MN)$ kernel matrix for gridding, $\mathbf{D}$ is the Fourier transform matrix, $\mathbf{Q}$ is the diagonal matrix performing the deapodization. The most commonly used kernel is the Kaiser-Bessel kernel [13] with a finite length which affects the accuracy and computational complexity of the regridding method.

Alternately, non-uniform fast fourier transform (NUFFT) can convert the nonuniform k-space measurements directly to uniform-grid image [15, 16]. Without the interpolation in k-space, the NUFFT method estimates the image by inverse NUFFT as

$$\hat{I}_n = \mathscr{F}^{-1}\{\mathbf{Pf}\} \tag{2}$$

www.manaraa.com

where $\mathscr{F}$ is the NUFFT operator [13, 14].

For the radial UTE measurement, we design the density compensation function for both regridding and NUFFT as

$$P(m) = \begin{cases} 0, & m = 1 \\ \lambda r_m \Delta_m + \beta, & m > 1 \end{cases} \tag{3}$$

where $P(m)$ is the $m$th diagonal element of the DCF matrix, $r_m = \sqrt{u_m^2 + v_m^2}$, $\Delta_m = \sqrt{(u_m - u_{m-1})^2 + (v_m - v_{m-1})^2}$, and $\lambda$ and $\beta$ are the parameters controlling the high-frequency and low-frequency weights, respectively.

www.manaraa.com

## 3. COMPRESSED SENSING FOR RADIAL MRI

When the sampling density $\eta = MN/L^2$ is less than 1, the image estimation problems (1) and (3) become under-determined and multiple solutions are possible. Compressed Sensing [11] is then used to exploit the sparsity of the image by solving a constrained L1 optimization problem. The regridding-CS becomes [12]

$$\hat{I}_g^{cs} = \underset{I}{\operatorname{argmin}} \frac{1}{2}||\mathbf{S}^{\star}\mathbf{D}\mathbf{Q}I - \mathbf{f}||_2^2 + \alpha_1||\mathbf{\Phi}I||_1 \tag{4}$$

Where $||\cdot||_p$ is the $p$th norm of a vector, $\alpha_1$ is the regularization parameter, $\mathbf{\Phi}$ is the sparsifying matrix, such as wavelet transform matrix, Discrete Cosine Transform (DCT) matrix, etc.

www.manaraa.com

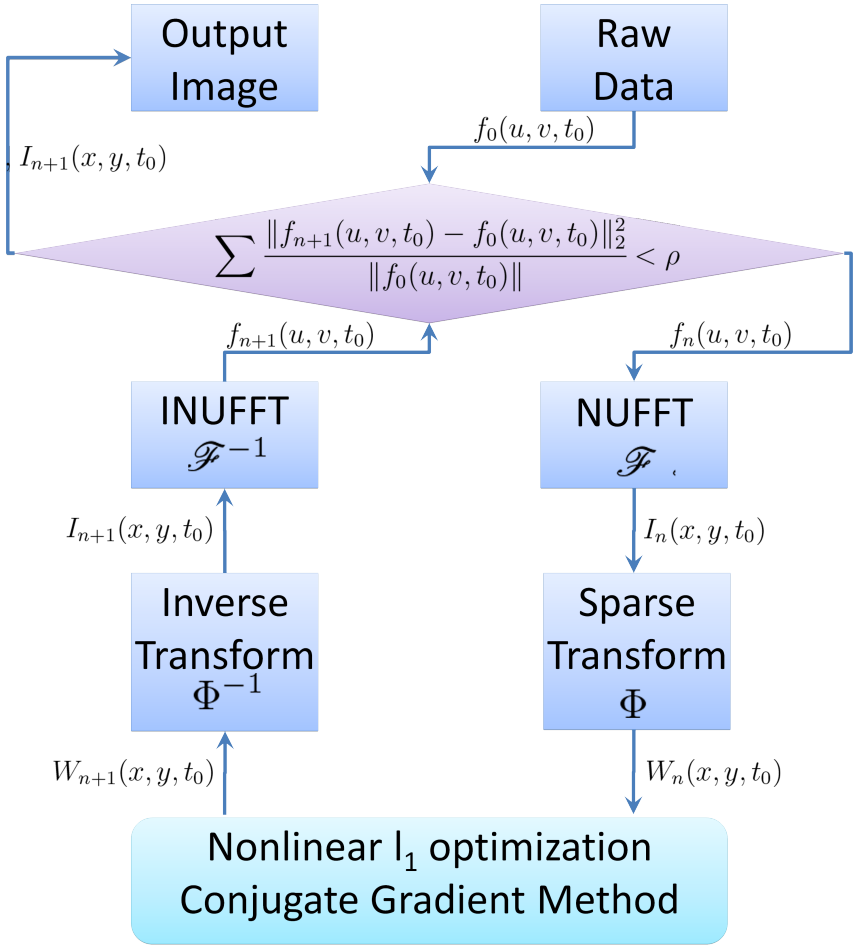


Figure 1: Block diagram of NUFFT-CS.

Combining the NUFFT method with the CS and adding the Total Variation (TV) constraint, we estimate the image as

$$\hat{I}_n^{cs} = \underset{I}{\operatorname{argmin}} \frac{1}{2}||\mathbf{P}^{-1}\mathscr{F}\{I\} - \mathbf{f}||_2^2 + \alpha_1||\mathbf{\Phi} I||_1 + \alpha_2 \mathrm{TV}(I) \tag{5}$$

Where $\mathrm{TV}(I)$ is the TV operator [3], and $\alpha_1$ and $\alpha_2$ are the weighting factors.

The nonlinear $l_1$-norm optimization (5) is solved iteratively by the conjugate gradient method [3], as shown in Figure 1, where the index $n$ denote the iteration, and the parameter $\rho$ is the stopping criterion.

www.manaraa.com

## 4. EXPERIMENTAL RESULTS

The radial MRI measurements were acquired for two samples a 7.0 T/ 20 cm Bruker AVANCE III BioSpec scanner. One sample was a phantom consisting of a Lego piece placed in a tube and another was a live mouse anesthetized by 2% isoflurane. In the phantom sample, a measurement with $N \times M = 128 \times 804$ radial readouts was acquired as the fully-sampled data set. The fully-sampled image was reconstructed by NUFFT with the size of the image being 256×256 in Cartesian grid. The under-sampled measurements were obtained from the fully-sampled measurement by keeping the first projection in every $d$ projects in the total of $N$ projections. The under-sampling rate is thus defined as $1/d$.

The animal sample was imaged as a gated cardiac MRI. The radial MRI scanning was triggered ECG signals measured by an SA Instrument ECG module. Three sets of scans were acquired with sizes as 97×610 as the fully-sampled measurement, 97×80 and 97×234 as the 13% and 38% undersampled measurements, respectively. All three scans had 40 frames in each cardiac cycle. The size of reconstructed images for the mouse cardiac sample was 194×194 in Cartesian grid.

The structure similarity (SSIM) index and the peak signal to noise ratio (PSNR) were to evaluate the quality of the reconstructed images. The SSIM between two images $I_1$ and $I_2$ is defined as:

$$\mathrm{SSIM}(I_1, I_2) = \frac{(2\mu_1\mu_2 + c_1)(2\sigma_{12} + c_2)}{(\mu_1^2 + \mu_2^2 + c_1)(\sigma_1^2 + \sigma_2^2 + c_2)} \tag{6}$$

where $\mu_1$ and $\mu_2$ are the means of $I_1$ and $I_2$, respectively, $\sigma_1^2$ and $\sigma_2^2$ are the variances of $I_1$ and $I_2$. respectively; $\sigma_{12}$ is the covariance of $I_1$ and $I_2$; $c_1 =$ and $c_2$ are two parameters to stabilize the division with weak denominator.

The PSNR (in dB) is defined as:

$$PSNR = 10 \log_{10} \frac{L^2 I_{MAX}^2}{\sum_{i=0}^{L-1} \sum_{j=0}^{L-1} [I_1(i,j) - I_2(i,j)]^2} \tag{7}$$

www.manaraa.com

where $I_1$ is the reference image, $I_2$ is the test image, $L \times L$ is the size of the images, and $I_{MAX}$ is the maximum value of image intensity. In our applications, $I_{MAX} = 255$.

Figure 2 shows the reconstructed images of the phantom sample, along with the intensity of the middle line of the images (at $x = 128$). On the left is the fully-sampled reconstruction by the NUFFT method which was used as the reference to compare other under-sampled reconstructions. The three columns of Figure 2 show the images reconstructed from 10%, 20% and 33% under-sampling rate, respectively. The three rows of Figure 2 show images reconstructed by ZF, NUFFT-CS and Regridding-CS, respectively. From the images, it is clear that the NUFFT-CS performed the best with the 30% reconstruction appearing almost exactly the same as the fully-sampled reconstruction. The 10% and 20% reconstructions exhibit little artifacts too. In contrast, the reconstructions by regridding-CS are filled with small noise and rings and the reconstructions from zero-filling are fuzzy and with significant artifacts, especially when the under-sampling rate is low. The smoothness of the intensity of the middle line curves also indicates the image quality. The middle line curves of the NUFFT-CS reconstructions are the smoothest among all the undersampled reconstructions and they resemble the middle line of the fully-sampled images well. In contrast, the noise and interference fluctuations inthe middle line curves of the regridding-CS and ZF are apparent degradation of the image quality.

Figure 3 shows the SSIM and PSNR of the undersampled reconstructions with reference to the fully sampled reconstruction. When the under-sampling rate is low, such as at 20% to 10% (or $d = 5 \sim 10$), the SSIM and PSNR of the NUFFT-CS are obviously higher than the ZF and regridding-CS. At the 10% undersampling rate, the NUFFT-CS has 0.2 higher SSIM and 8 dB higher PSNR than those of the ZF reconstructions. The SSIM and PSNR of the regridding-CS are low at all sampling rates, which indicates that the regridding method is ineffective to CS optimization.

Figure 4 shows the reconstructed images of the first frame of the 40 mouse cardiac frames. Again, the reconstruction by NUFFT with fully-sampled measurement, as shown

www.manaraa.com

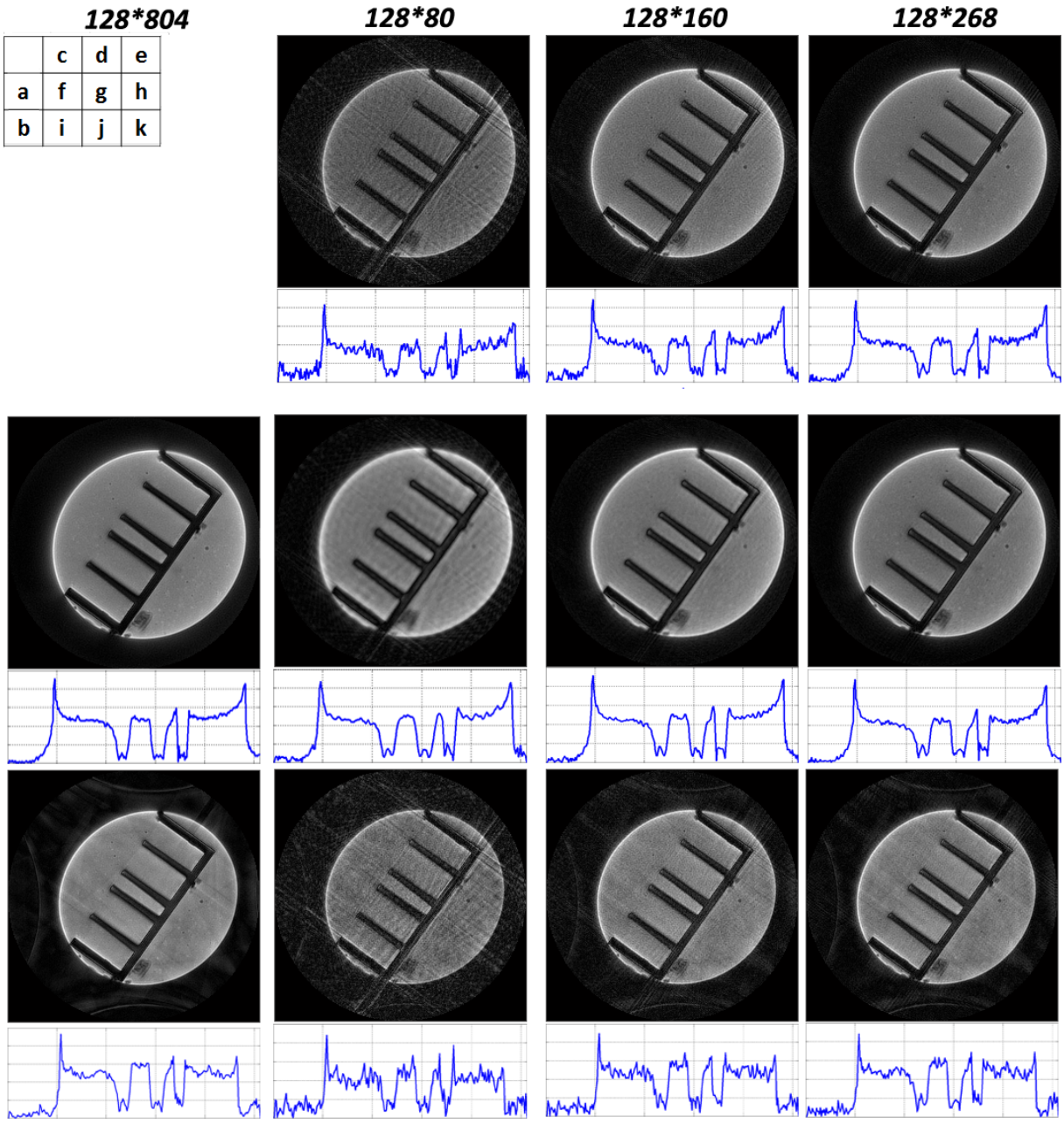


Figure 2: Reconstructed images and their middle line intensity curves of the phantom. (a) fully-sampled, NUFFT. (b) fully-sampled, regridding. (c)-(e) under-sampled, zeros-filling. (f)-(h) under-sampled, NUFFT-CS. (i)-(k) under-sampled, regridding-CS.

in Figure 4(a), is used as the reference image for quality evaluation of the undersampled reconstructions. The two columns on the right in Figure 4 show the images reconstructed from 97×80 and 97×234 under-sampled measurement respectively. The three rows show

www.manaraa.com

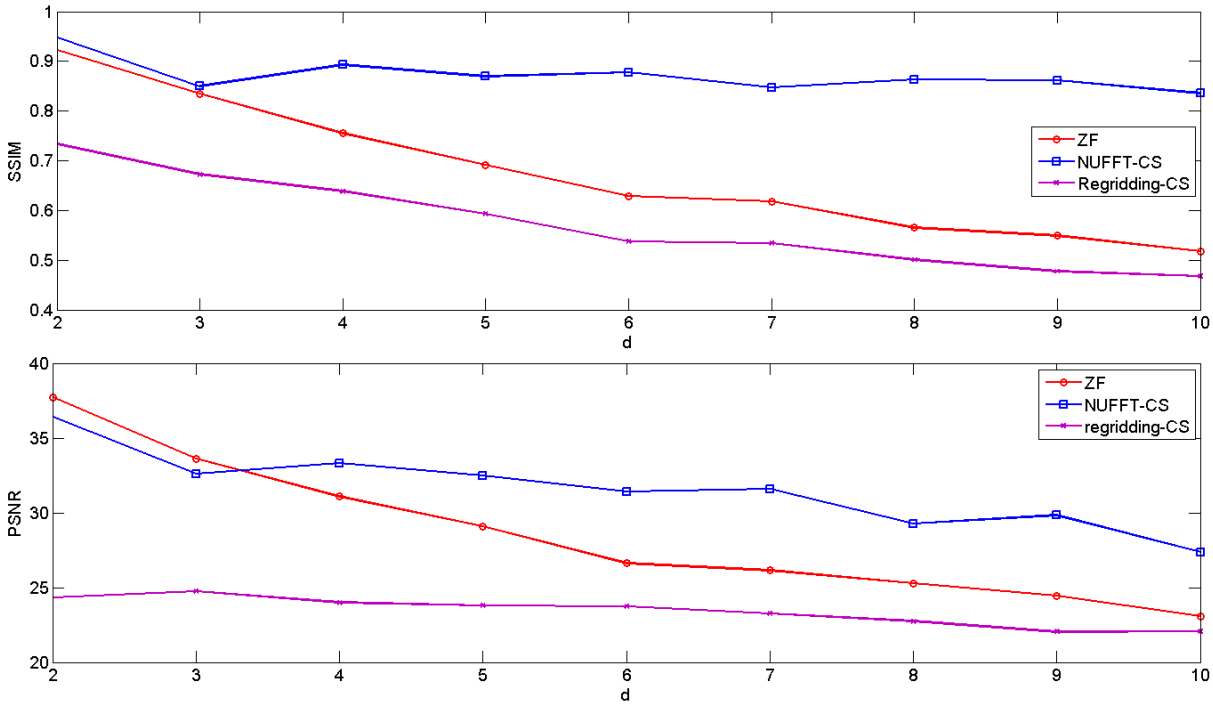


Figure 3: SSIM and PSNR of the phantom images reconstructed from different under-sampling rates. Note the undersampling rate is $100/d$ percent.

the image reconstructed by ZF, NUFFT-CS and Regridding-CS, respectively. The ZF reconstructions suffer from strong noise and blurry degradation. The NUFFT-CS reconstructions are clear and smooth. The regridding-CS reconstructions are filled aliasing artifacts. With the 13% undersampling rate, the reconstruction of the NUFFT-CS is useable while the reconstructions from ZF and regridding-CS are unacceptable. With the 38% undersampling rate, the reconstruction of the NUFFT-CS differs clearly from the fully-sampled reconstruction. This is rather different from the results in the phantom sample, because the undersampling experiments were conducted after the full-sampling experiment so the mouse heart beats were at different times and the images can be slightly different. In fact, the total number of cardiac cycles required for acquiring 80 projections is a lot less than the total number of cycles to acquire 610 or 234 projections. Therefore, we see less artifacts in Figure 4(d) than in Figure 4(e) and (a).

www.manaraa.com

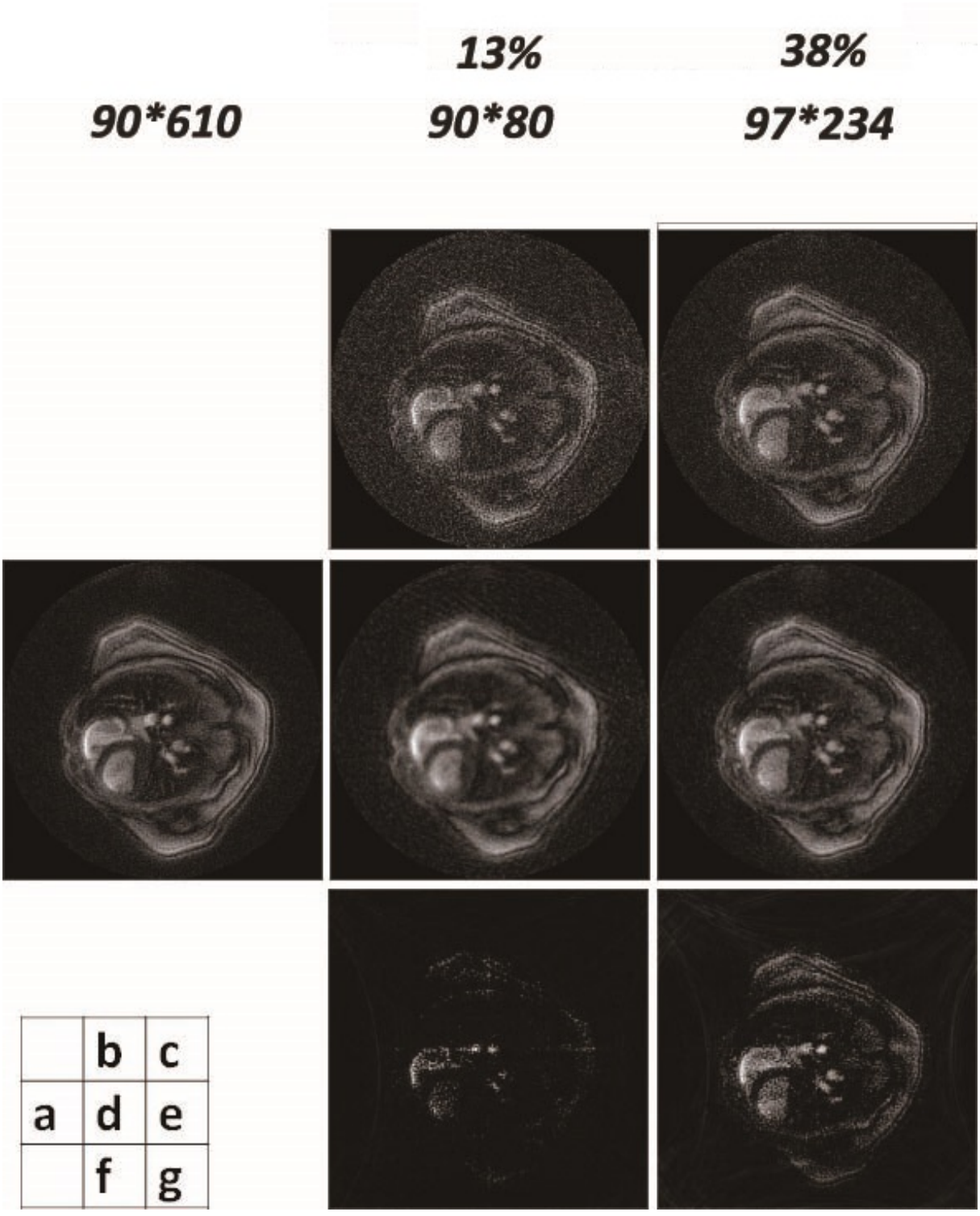


Figure 4: Mouse cardiac radial MRI reconstructions. (a) fully-sampled, (b)-(c) under-sampled, zero-filling (d)-(e) under-sampled, NUFFT-CS. (f)-(g) under-sampled, regridding-CS.

www.manaraa.com

Table 1 shows the SSIM and PSNR of the under-sampled reconstructions in reference to the fully-sampled reconstructions. The results are much less than those of the phantom sample. This is mainly because the reference image may not be the ground truth for comparison. Since the animal was alive and the heart beats were unnecessarily the same in each cycle due to abdominal movement, the images reconstructed from multiple cycle measurements can suffer significantly from the artifacts. Nevertheless, the advantages of NUFFT over the ZF and regridding-CS are still obvious from Table 1. If we take the fully-sampled data and electronically throw away some projections, as done in the phantom sample, then the SSIM and PSNR results are similar to those shown in Figure 3.

Table 1: SSIM and PSNR of reconstructions from under-sampled mouse cardiac sample.

| | | NUFFT-CS | Zero-filling | Regrid-CS |
|---|---|---|---|---|
| 13% | PSNR | 26.2 dB | 20.9 dB | 15.4 dB |
| | SSIM | 0.59 | 0.38 | 0.16 |
| 38% | PSNR | 25.7 dB | 23.8 dB | 14.6 dB |
| | SSIM | 0.56 | 0.48 | 0.14 |

From the results of the two samples, we conclude that the NUFFT-CS approach significantly improves the quality of the reconstructions at low sampling rates. While it can be used for radial MRI reconstruction of fully-sampled measurement, regridding used in CS reconstruction suffers from large errors and the L1 optimization is difficult to converge. Regridding-CS performs even worse than the zero-filling algorithm for low undersampling rates.

www.manaraa.com

## 5. ACKNOWLEDGMENT

The work was supported by the Inter-Discipline Inter-Campus program of University of Missouri and the Intelligent System Center of Missouri University of Science and Technology.

www.manaraa.com

## II. AUTOMATED CARDIAC SELF-GATED RADIAL CMRI

Xiahan Yang, Yahong Rosa Zheng, and Lixin Ma

**ABSTRACT**—Distortions in electrocardiogram (ECG) signals affect the image quality and increase scan time of Cardiac Magnetic Resonance Imaging (CMRI) exams. This study proposes an alternative method of acquiring CMRI cine images in mouse heart using a self-gated Ultra-short Echo Time (UTE) protocol. In our method, a bandpass filter and a lowpass filter are adopted to extract the self-gated signals from the center of the raw no-gated k-space measurements, A live mouse has been tested as the example to verify the method. The results demonstrated that this method could be used for reconstruction of the no-gated UTE CMRI measurements without using of external ECG signals.

www.manaraa.com

# 1. INTRODUCTION

Cardiac Magnetic resonance imaging (CMRI) of the beating heart is commonly acquired by electrocardiogram (ECG) and respiratory triggering. The need of an ECG equipment results in additional complexity for CMRI exam. Furthermoredistortions and artifacts in ECG signals generated by the MR scanner affect the image quality and increase the scan time during the CMRI exam [17] [18]. Few self-gated (SG) methods have been proposed to replace the ECG triggering acquisition including self-gated Fast Low Angle SHot (FLASH) CMRI [19] [20]. However, the current self-gated methods are not robust, especially for radial k-space acquisition pulse sequences. Ultra-short echo time (UTE) CMRI technology. With the Ultra-short Echo Time (UTE) imaging sequence is a new ultrafast radial k-space sequence that can significantly reduce flow-artifacts, and achieve high image quality in the fast beating murine heart. A robust self-gated UTE acquisition and reconstruction method is of interest to the field.

The basic idea of self-gating is extracting the information of cardiac cycle from the k-space measurements without extra operators or equipment [21]. Some researcher are working on the respiratory self-gated research [5] [6] [22]. Though the complexity and scan time have been reduced with the respiratory gated methods, there is still an apparent gap with the methods, where respiratory-gated methods still depend on the external devices and the waiting time still exists.

There are three difference directions to extract the self-gated signal information from the radial k-space measurement [5]. First is named as k0-line checking. Only the first element in each projection is processed to extract the information of cardiac cycle. Second is named as k1-line checking. Different from the first method, k1-line checking will apply the whole k-space measurements to extract the information of cardiac cycle. The last one is named as image checking. Instead of ejecting the information of cardiac cycle from the k-space measurements, this method will extract the information from the reconstructed CMR image.

www.manaraa.com

In our research, we applied the k0-line method for its balance of complexity and accuracy. The accuracy of the self-gated signals is ensured by a bandpass filter designed with the sample animal cardiac characteristics. We also applied some restrictions named as peak-detection to further improve the accuracy. The raw no-gated radial measurements is resorted by the self-gated signals before reconstruction. The non-uniform Fast Fourier transform (NUFFT) algorithm [14] was applied to transform the sorted data to the image domain instead of the traditional regridding method. The NUFFT approach effectively improve the quality of the reconstruction. The cardiac images rebuilt from the sorted data could be distinguished with clear phase different.

www.manaraa.com

## 2. CARDIAC CYCLE DETECTION METHOD

The information of cardiac cycle can be obtained through the raw no-gated radial measurement. As the radial CMRI measurement, set as $\mathbf{S}(\mu, \phi)$ is calculated in the frequency domain, also known as k-space, frequency analysis is a good entry point. The center of the k-space represents the lowest frequency part. In the radial measurements, the data located in the center of k-space is recorded in the first elements in each projection which is set as $\mathbf{k_0}(\phi)$. Proven from the 2-D frequency theory, the lowest frequency part in the image domain is the smoothest part in the image domain. In the mouse cardiac image, left and right ventricular (LV and RV) are obviously the smoothest part in cardiac image as signals from other tissues and muscles are much smaller than them. Coincidentally, the cardiac cycle is also exhibited by the LV and RV ejection and inflow. As a result, we can use the $\mathbf{k}_0(\phi)$ which is defined in Eq.1 to extract the information of cardiac cycle which could rebuild the self-gated signal used to reconstruct the dynamic cardiac images.

$$\mathbf{k}_0(\phi) = \mathbf{S}(0, \phi), \phi \in \{0, N_{movie} - 1\} \tag{1}$$

where $\phi$ is the order of projections $N_{movie}$ is the number of frames set in MRI exam.

Here is the brief introduction of extracting the end-diastolic (when the heart is the largest) point $\mathbf{p}$ from the $\mathbf{k_0}(\phi)$. In our research, the magnitude $|\mathbf{k}_0(\phi)|$ is applied to extract the self-gated signals since the raw data are complex value. Experiments have proven that the performances of other mathematical transformations such as real part $Real()$, imagine part $Imag()$, phase $\Theta$, etc. are equal or worse than the magnitude. As the $\mathbf{k}_0(\phi)$ is filled with kinds of noises and measurement error. Filter is necessary to eliminate the noise and improve the accuracy in the self-gated signals detection using Eq.2.

$$\mathbf{g} = \mathbf{h} \otimes \mathbf{k}_0(\phi) \tag{2}$$

www.manaraa.com

where $\mathbf{g}$ is the raw self-gated signals and $\mathbf{h}$ is the filter.

The peaks on the $\mathbf{g}$ are the candidates of the end-diastolic (ED) point or the self-gated signals $\mathbf{p}$ in the cardiac cycle as proved. First, we calculated all the maximum points in $\mathbf{g}$. It should be noted that with noise and measurements errors, not all the peaks are the accurate ED point. Restrictions based on the characteristic of mouse cardiac cycle are applied to select the accurate ED points as the last procedures in self-gated signal extraction . These selected ED points are considered as the ED phases and are applied in resorting the raw no-gated measurements. Figure 1 shows the procedures to generate the SG-signal.

As shown in Eq.1 and Eq.2, filter is an important parameter. In our research, we compared two different kinds of filters to obtain the raw self-gated signal. The lowpass filter and the bandpass filter, the lowpass filter is designed to reduce the high frequency noise in the $\mathbf{k_0}(\phi)$ instead of just extracting the cardiac cycle frequency. Combined with the characteristics of mouse heart, The bandpass filter is designed to intercepts the exactly cardiac cycle frequency band.

The lowpass filter is a simple model. Since it is only designed to eliminates the high frequency noise, the normalized cut-off frequency is set to $2\pi \times 0.9$ without an exactly calculation.

On the other hand, the bandwidth filter is much more complex. Since the heart rate for mouse or other animals should have a range and let set it to $[B_{min}, B_{max}]$ beat per minute (bpm). Converting it to Hertz (Hz), the mouse cardiac cycle is in the range of $[B_{min}, B_{max}]60Hz$. And as in the $\mathbf{k_0}(\phi)$, the interval between two points is the repetition time (TR) in the CMRI sequence, set it to $T_r$ . To extract the information of cardiac cycle, we build a bandpass filter with the $[B_{min}, B_{max}] \times T_r \times \pi 60]$ pass band which is the range of cardiac cycle frequency. The peaks of the signal $\mathbf{g}$ should represent the end-diastolic cardiac phase when the LV and RV are in the largest phase which shows as one peak in the $\mathbf{k_0}(\phi)$. Then it is easy to rebuild the self-gated signal $\mathbf{p}$ by extracting the peaks.

www.manaraa.com

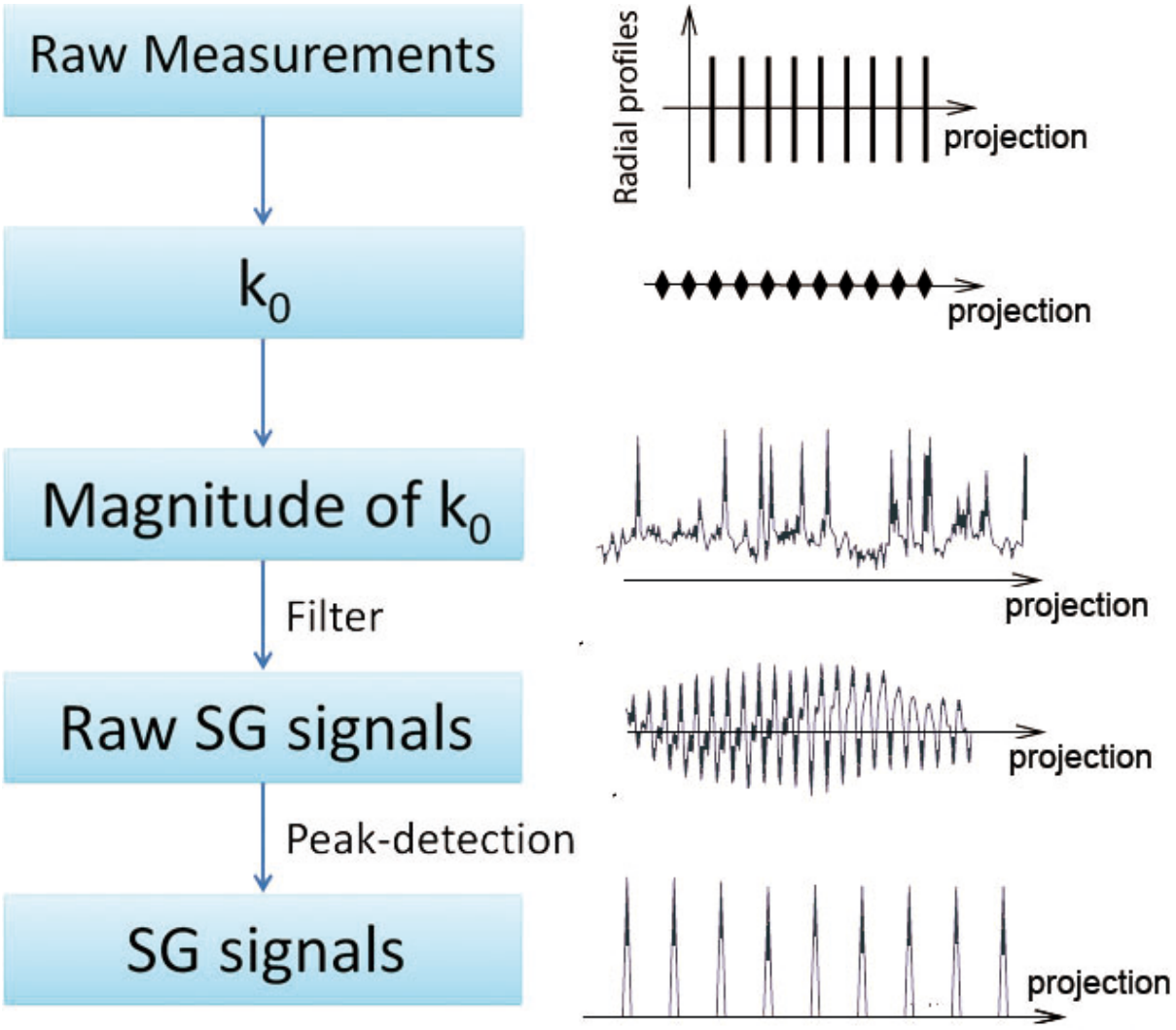


Figure 1: Overview of the generation of self-gated signals $\mathbf{g}$.

The end-diastolic points belong to a subset of the peaks of the curves of raw self-gated signals. As mentioned above, the center of the k-space measurements represent the ventricle signals in image domain. The peaks could be viewed as the moments when the LV is in the largest area or the end-diastole. However, the heart beat is not uniform all the time, and there exist noises and measurement errors, few peaks collected in the raw self-gated signals do not represent the ED point and some ED points have been covered in the raw self-gated signals. It is necessary to do further detection.

www.manaraa.com

The restrictions applied to peak-detection which is automated, are mainly based on the cardiac characteristics. First as the mouse cardiac cycle is in the range of 350 $\sim$ 550 bpm, and the TR in UTE method is 8.5 ms, the distance between two peaks should be in the range of 10 $\sim$ 25 frames. The peak whose distance from the neighborhood exceeds this range should be ignored. Second, we set a threshold to delete the low peaks where most of them are the results of noise. The initial value of the threshold is 0.8 times the maximum peak value. This value would be adjusted during calculation to preserve normal number of peaks which is based on the mouse cardiac cycle range and the scanning time in one phase-encoding direction.

Raw no-gated measurements between two peaks would be resorted to the re-designed cardiac frames before reconstruction. As the lengthes between two peaks would not be exactly as same as the pre-set cardiac frames, interpolating is applied to fix the length and reshift the measurements to the correct frames.

www.manaraa.com

## 3. EXPERIMENTAL RESULTS

The UTE no-gated CMRI measurements were acquired on a 7.0T/ 20 cm Bruker AVANCE III BioSpec scanner equipped with a 35 mm inner-diameter volume RF coil. A female CF1 live mouse with 4 months of age and 26 g of body weight was anesthetized by 2% isoflurance in oxygen. The animal was imaged using as a no-gated UTE CMRI sequence. Table.1 shows the details of the CMRI exam.

Table 1: No-gated CMRI exam parameters for live animal.

| TR | TE | $N_{movie}$ |
|---|---|---|
| 8.5 ms | 0.402 $\mu$s | 80 |
| NA | Estimated time | Elapsed time |
| 1 | 5m18s | 5m33s |

In Table.1, TR is repetition time, TE is echo time, $N_{movie}$ is the number of frames, NA is the number of average. From the table, we can see that the elapsed time is just 15 s larger than the estimated time. Compared with the ECG method where the elapsed time is always more than 7 minutes with this set of parameters, the no-gated UTE method saves significant scan time.

However, the highly similarity of different frames reconstructed from the raw no-gated radial measurement conceals the cardiac beating information. The following text will show the results of the reconstructions for the resorted measurements by the self-gated signal extracted from the original data.

The Self-gated filter is the most important part of self-gating detector. Figure 2 shows the frequency responses of the two kinds of filters: bandpass filter and lowpass filter which are applied in the no-gated images, respectively. The bandpass range was 5 $\sim$ 10 Hz, based on the pretext derivation and the mouse cardiac rate. The order is 201

www.manaraa.com

and the stop-band attenuation was set to 30 dB. The lowpass range was $0 \sim 85$ Hz. The order of lowpass filter was 101 and the attenuation was 30 dB.

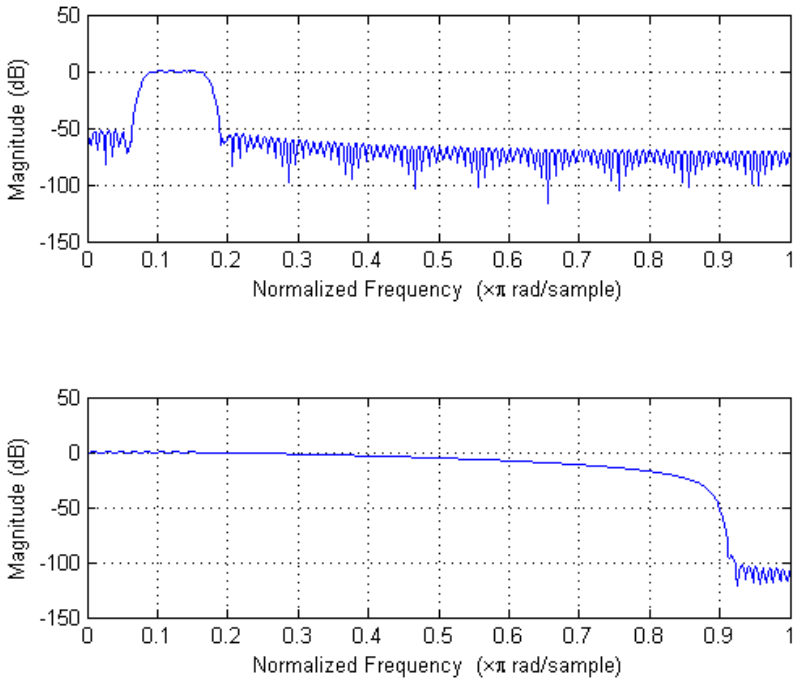


Figure 2: The frequency response of bandpass and the lowpass filters applied in the no-gated UTE CMRI measurements to extract the information of cardiac cycle.

Figure 3 shows the raw self-gated signals $\mathbf{g}$ and the chosen peaks $\mathbf{p}$. Limited by the space, only four projections have been exhibited: $1^{st}$, $21^{st}$, $41^{st}$ and $101^{st}$. The order of the projection is shown on the top of each sub-figure. The horizonal axis represents the order of movie and the vertical axis represents the normalized magnitude value. The 'o' in the curves represents the end-diastolic peak after the detection.

To rebuild images from the radial CMRI measurements, NUFFT is adopted instead of the traditional FFT. NUFFT can convert the nonuniform k-space measurements directly to uniform-grid image. Without the interpolation in k-space, the NUFFT method

www.manaraa.com

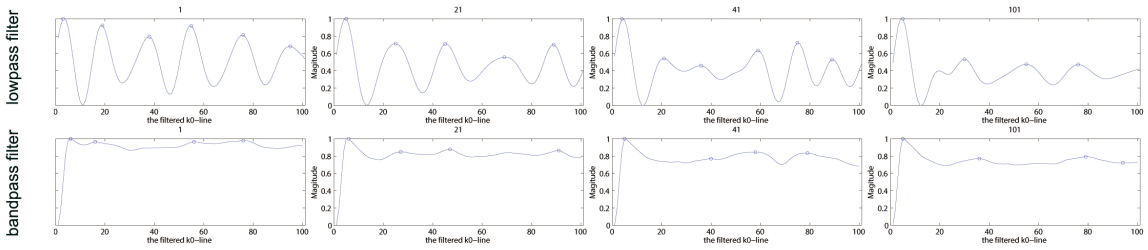


Figure 3: The raw self-gated signals $\mathbf{g}$ and peaks $\mathbf{p}$ checked with the Peak-detection restrictions.

estimates the image by inverse NUFFT as

$$\hat{I}_n = \mathscr{F}^{-1}\{\mathbf{Df}\} \tag{3}$$

where $\mathscr{F}$ is the NUFFT operator, $\mathbf{D}$ is the density compensation function introduced later and $\mathbf{f}$ is the resorted radial CMRI measurements based on the self-gated signals $\mathbf{p}$.

Figure 4 shows the final reconstructions which are rebuilt from the reshifted measurements by the self-gated signals with two different filter. The first row is the results from the bandpass filters and the second row is the results from the lowpass filters. The far left column exhibits the end-diastolic cardiac phase. The following is the ejecting, end-systolic inflowing and back to end-diastolic phases.

www.manaraa.com

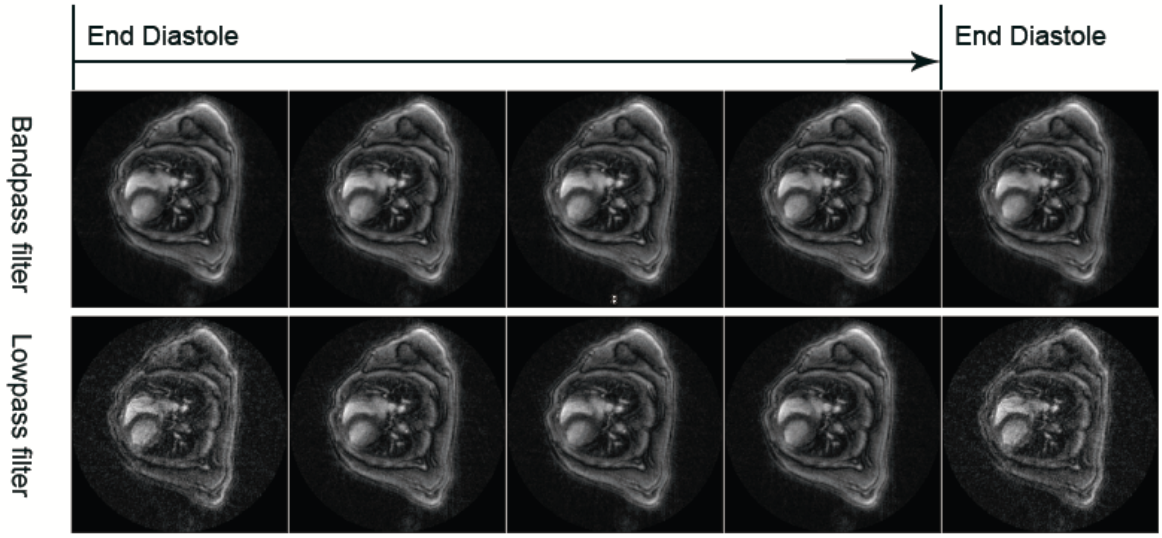


Figure 4: The reconstructions from the resorted k-space measurements.

From the Figure 3 and Figure 4, the improvement of the bandpass filter is apparent. In Figure 3, the curve of $\overline{\mathbf{G}}$ could more effectively exhibit the cardiac cycle subjectively. The accuracy of the peak detection is also ensured by the clear curves. The images reconstructed with bandpass filter are also clearer than the ones reconstructed with lowpass filter. Noises and artifacts have been significantly reduced with the bandpass filter. The contrast between the ventricular and other tissues has also been increased with the bandpass filter. In a conclusion, bandpass filter can accurately extract self-gated signals. The reconstructions with bandpass filter can effectively distinguish the cardiac cycle.

www.manaraa.com

# 4. CONCLUSION

In this paper, we reconstructed mouse cardiac images from self-gated radial UTE measurements. We adopted a bandpass filter with peak-detection restrictions to extract the self-gated signals. We also compared results with a common lowpass filter. Both of the reconstructions and the self-gated signals quality has been improved. The reconstructions with bandpass filter can effectively distinguish the cardiac cycle where the MRI exam time and the radiations have been significantly reduced.

Possible directions of research include combining the Compressed Sensing (CS) technology with the Self-Gated to reduce the MRI exam time much more obviously, where the Compressed Sensing could reconstructed signals from an under-sampling measurements.

www.manaraa.com

## 5. ACKNOWLEDGMENT

The work was supported by the Inter-Discipline Inter-Campus program of University of Missouri and the Intelligent System Center of Missouri University of Science and Technology.

www.manaraa.com

# SECTION

# 2. CONCLUSION

Ultra-short echo time (UTE) as a new technology proposed in recent year, improve the quality of the MRI quality while also bring some unsolved problems. The increasing of the scanning time is one of the major issue. In our project, we proposed two approaches reducing the UTE MRI scanning time: NUFFT-CS and Self-Gating. To verify our theory, sample measurements and real animal measurements are applied. Based on the results of the measurements, we conclude that the NUFFT-CS approach significantly improves the quality of the reconstructions at low sampling rates. Compared with the conventional Regridding algorithm and the directly zero-filling (ZF) approaches, the advantages of NUFFT-CS are obvious from the objective image assessment. Based on the NUFFT-CS approach, the amount of the measurements needed in MRI exam is high reduced, the scanning time of MRI exam is shorten significantly and the quality of the reconstructions is keeping in high level.

Instead of reducing the number of measurement trajectories, we apply self-gating in order to eliminate the waiting time in the ECG trigger MRI. Based on the cardiac cycle information from the UTE measurements, we reconstructed mouse cardiac images successfully with a bandpass filter. Compared the results with a common lowpass filter, both of the reconstructions and the self-gated signals quality has been improved. The reconstructions with bandpass filter can effectively distinguish the cardiac cycle where the MRI exam time and the radaitions have been significantly reduced.

www.manaraa.com

# BIBLIOGRAPHY


[1] M. D. Robson, P. D. Gatehouse, M. Bydder, and G. M. Bydder, "Magnetic resonance: an introduction to ultrashort te (ute) imaging," *Journal of computer assisted tomography*, vol. 27, no. 6, pp. 825–846, 2003.

[2] A. G. Motaal, B. F. Coolen, D. Abdurrachim, R. M. Castro, J. J. Prompers, L. M. Florack, K. Nicolay, and G. J. Strijkers, "Accelerated high-frame-rate mouse heart cine-MRI using compressed sensing reconstruction," *NMR in Biomedicine*, vol. 26, no. 4, pp. 451–457, 2013.

[3] M. Lustig, D. Donoho, and J. M. Pauly, "Sparse MRI: The application of compressed sensing for rapid MR imaging," *Magnetic Resonance in Medicine*, vol. 58, no. 6, pp. 1182–1195, 2007.

[4] M. Lustig, D. L. Donoho, J. M. Santos, and J. M. Pauly, "Compressed sensing mri," *Signal Processing Magazine, IEEE*, vol. 25, no. 2, pp. 72–82, 2008.

[5] J. Paul, E. Divkovic, S. Wundrak, P. Bernhardt, W. Rottbauer, H. Neumann, and V. Rasche, "High-resolution respiratory self-gated golden angle cardiac MRI: Comparison of self-gating methods in combination with k-t SPARSE SENSE," *Magnetic Resonance in Medicine*, 2014.

[6] B. Hiba, N. Richard, M. Janier, and P. Croisille, "Cardiac and respiratory double self-gated cine mri in the mouse at 7 t," *Magnetic resonance in medicine*, vol. 55, no. 3, pp. 506–513, 2006.

[7] Y. Zhang, H. P. Hetherington, E. M. Stokely, G. F. Mason, and D. B. Twieg, "A novel k-space trajectory measurement technique," *Magnetic Resonance in Medicine*, vol. 39, no. 6, pp. 999–1004, 1998.

[8] M. D. Robson and G. M. Bydder, "Clinical ultrashort echo time imaging of bone and other connective tissues," *NMR in Biomedicine*, vol. 19, no. 7, pp. 765–780, 2006.

[9] H. Sedarat and D. G. Nishimura, "On the optimality of the gridding reconstruction algorithm," *IEEE Trans. Medical Imaging*, vol. 19, no. 4, pp. 306–317, 2000.

[10] J. D. O'Sullivan, "A fast sinc function gridding algorithm for fourier inversion in computer tomography," *IEEE Trans. Medical Imaging*, vol. 4, no. 4, pp. 200–207, 1985.

[11] D. L. Donoho, "Compressed sensing," *IEEE Trans. Information Theory*, vol. 52, no. 4, pp. 1289–1306, 2006.

[12] S. Nam, M. Akçakaya, T. Basha, C. Stehning, W. J. Manning, V. Tarokh, and R. Nezafat, "Compressed sensing reconstruction for whole-heart imaging with 3D radial trajectories: A graphics processing unit implementation," *Magnetic Resonance in Medicine*, vol. 69, no. 1, pp. 91–102, 2013.


www.manaraa.com

[13] L. Greengard and J. Y. Lee, "Accelerating the nonuniform fast fourier transform," *SIAM review*, vol. 46, no. 3, pp. 443–454, 2004.

[14] J. A. Fessler, "On NUFFT-based gridding for non-Cartesian MRI," *Journal of Magnetic Resonance*, vol. 188, no. 2, pp. 191–195, 2007.

[15] H. Kajbaf, J. T. Case, Z. Yang, and Y. R. Zheng, "Compressed sensing for sar-based wideband three-dimensional microwave imaging system using non-uniform fast fourier transform," *IET Radar, Sonar & Navigation*, vol. 7, no. 6, pp. 658–670, 2013.

[16] Z. Yang and Y. R. Zheng, "A comparative study of sparse methods for 3-d synthetic aperture radar image reconstruction," *Elsevier DSP*, vol. 32, pp. 24–33, 2014.

[17] R. N. Dimick, L. W. Hedlund, R. J. Herfkens, E. K. Fram, and J. Utz, "Optimizing electrocardiograph electrode placement for cardiac-gated magnetic resonance imaging." *Investigative radiology*, vol. 22, no. 1, pp. 17–22, 1987.

[18] A. A. Damji, R. E. Snyder, D. C. Ellinger, F. X. Witkowski, and P. S. Allen, "RF interference suppression in a cardiac synchronization system operating in a high magnetic field NMR imaging system," *Magnetic Resonance Imaging*, vol. 6, no. 6, pp. 637–640, 1988.

[19] S. Uribe, V. Muthurangu, R. Boubertakh, T. Schaeffter, R. Razavi, D. L. Hill, and M. S. Hansen, "Whole-heart cine mri using real-time respiratory self-gating," *Magnetic Resonance in Medicine*, vol. 57, no. 3, pp. 606–613, 2007.

[20] M. E. Crowe, A. C. Larson, Q. Zhang, J. Carr, R. D. White, D. Li, and O. P. Simonetti, "Automated rectilinear self-gated cardiac cine imaging," *Magnetic Resonance in Medicine*, vol. 52, no. 4, pp. 782–788, 2004.

[21] V. Hoerr, N. Nagelmann, A. Nauerth, M. T. Kuhlmann, J. Stypmann, and C. Faber, "Cardiac-respiratory self-gated cine ultra-short echo time (UTE) cardiovascular magnetic resonance for assessment of functional cardiac parameters at high magnetic fields," *Journal of Cardiovascular Magnetic Resonance*, vol. 15, no. 1, p. 59, 2013.

[22] C. Santa Marta, M. Ledesma-Carbayo, A. Bajo, E. Pérez-David, A. Santos, and M. Desco, "Respiratory gated spamm sequence for magnetic resonance cardiac tagging," in *Computers in Cardiology, 2006.* IEEE, 2006, pp. 61–64.

www.manaraa.com

# VITA

Xiahan Yang was horn on July $12^{th}$, 1993 in Beijing, China. He received his Bachelor of science in Electronics Engineering from Tianjin University, Tianjin, China in 2009. In May, 2015, he received his M.S. in Electrical Engineering from Missouri University of Science and Technology. And then continue his study for a Ph.D. degree in the Missouri University of Science and Technology, Rolla, MO. His research interests are digital image processing, compressed sensing and image assessment.

www.manaraa.com